Molecular Neurobiology (2019) 56:8136–8156
https://doi.org/10.1007/s12035-019-01654-1

Autophagy Stimulation Decreases Dopaminergic Neuronal Death Mediated by Oxidative Stress

Marcela J. Ramirez-Moreno[1] · Ana P. Duarte-Jurado[1] · Yareth Gopar-Cuevas[1] · Alfredo Gonzalez-Alcocer[1] · Maria J. Loera-Arias[1] · Odila Saucedo-Cardenas[1,2] · Roberto Montes de Oca-Luna[1] · Humberto Rodriguez-Rocha[1] · Aracely Garcia-Garcia[1]

Received: 7 February 2019 / Accepted: 17 May 2019 / Published online: 13 June 2019

Abstract

The neurodegenerative process of Parkinson's disease (PD) involves autophagy impairment and oxidative stress. Therefore, we wanted to determine whether stimulation of autophagy protects dopaminergic cell death induced by oxidative stress in a PD model. Since environmental exposure to herbicides increases the risk to develop PD, the experimental model was established using the herbicide paraquat, which induces autophagy disruption, oxidative stress, and cell death. Rapamycin-stimulated autophagy inhibited calpain-dependent and independent apoptosis induced by paraquat. Autophagy stimulation decreased oxidative stress and peroxiredoxins (PRXs) hyperoxidation induced by paraquat. Cells exposed to paraquat displayed abnormally large autophagosomes enclosing mitochondria, which correlates with an increase of p62, an essential mitophagy regulator. Interestingly, when autophagy was stimulated before paraquat treatment, autophagosome size and number were similar to that observed in control cells. Motor and cognitive function impairment induced by paraquat showed an improvement when preceded by autophagy stimulation. Importantly, dopaminergic neuronal death and microglial activation mediated by paraquat were significantly reduced by rapamycin-induced autophagy. Our results indicate that autophagy stimulation has a protective effect on dopaminergic neurons and may have a promising potential to prevent or delay PD progression.

Keywords Autophagy · Oxidative stress · Paraquat · Parkinson's disease · Rapamycin

Introduction

Parkinson's disease (PD) is characterized by the dopaminergic neuronal loss in the *substantia nigra* at the central nervous system (CNS), a significant reduction in dopamine levels affecting the motor function, and the presence of Lewy bodies [1, 2]. Most of the PD cases have an idiopathic origin, but it is believed that genetic susceptibility, environmental exposures, and aging concur in the progress of this disease [3, 4]. Epidemiological studies have demonstrated that environmental exposures to herbicides and pesticides increase the risk of developing PD [5–8]. Although the underlying etiology of PD is not entirely understood, several mechanisms have been associated with promoting neuronal death, including mitochondrial dysfunction, oxidative stress, and protein accumulation [9–11]. The latter is related to the main pathological hallmark of PD, the presence of Lewy bodies, which are composed of abnormal deposits of protein aggregates, particularly α-synuclein and ubiquitin-bound proteins [12]. Abnormal protein aggregation results from the proteasome and autophagy alteration, and in the latter, includes disruption of lysosomal hydrolase trafficking [13–15]. Importantly, both degradation pathways are dysregulated or inhibited in PD [16].

Autophagy is a self-regulatory mechanism involving macromolecules and organelles degradation, which are sequestered into autophagosomes [17, 18]. Ulterior fusion with a

Electronic supplementary material The online version of this article (https://doi.org/10.1007/s12035-019-01654-1) contains supplementary material, which is available to authorized users.

✉ Aracely Garcia-Garcia
aracely.garciagr@uanl.edu.mx

[1] Departamento de Histologia, Facultad de Medicina, Universidad Autonoma de Nuevo Leon, Francisco I. Madero S/N, 64460 Monterrey, Nuevo Leon, Mexico

[2] Departamento de Genética Molecular, Centro de Investigación Biomédica del Noreste, Instituto Mexicano del Seguro Social, Delegación Nuevo León, , Mexico

lysosome leads to their degradation by hydrolases, and the byproducts can be re-used for cell survival [19, 20]. In the last decade, the fundamental role of autophagy in neuronal homeostasis has been demonstrated, as its disruption leads to neurodegeneration [21, 22]. Specific depletion of *Atg5* and *Atg7* in the CNS caused motor and behavioral alterations, aggregation of polyubiquitinated proteins forming inclusions in neurons, and massive neuronal loss [21–24]. Importantly, postmortem brain samples of PD patients showed the abnormal presence of autophagy intermediaries (autophagosomes and autolysosomes) [25, 26].

The herbicide paraquat reproduces many of the characteristics of PD including mitochondrial dysfunction, oxidative stress, autophagy disruption, and cell death [27–30]. Indeed, paraquat toxicity is mediated by oxidative stress, particularly, in the mitochondria [27]. Additionally, autophagy impairment enhanced the toxicity mediated by paraquat, while its stimulation reduced this effect [28]. Controversially, autophagy can be either induced or inhibited by oxidative stress. Low levels of reactive oxygen species (ROS) are essential for many cellular processes, including autophagy, where autophagosome formation depends on ATG4 oxidation [31]. Another study reported that besides mitochondria, autophagosomes and lysosomes are main compartments for basal ROS production [32]. Also, autophagy induced by starvation is regulated by superoxide anion (O_2^-), while its inhibition occurs by overexpression of manganese superoxide dismutase (Mn-SOD), which scavenges O_2^- [33]. On the other hand, oxidative stress induced lysosomal membrane protein aggregation through thiol groups cross-linkage, which leads to disruption of lysosomal function by increasing its proton permeability capacity, with a subsequent pH rise and acidic hydrolases inactivation [34]. Interestingly, *ATG5* and *ATG10* knockdown increased ROS induced by starvation [35], which suggests a protective role of autophagy against oxidative stress.

Since we have observed that paraquat inhibits autophagy, and by inducing autophagy with rapamycin, dopaminergic cell death is reduced; we aimed to determine the impact of autophagy stimulation on dopaminergic neuronal cell death-induced by oxidative stress and whether it can be reproduced in vivo. We established the experimental cellular and animal model of PD using paraquat. Autophagy stimulation decreased both calpain-dependent and independent apoptosis induced by paraquat. Autophagy inhibited oxidative stress and peroxiredoxins (PRXs) hyperoxidation induced by paraquat. Also, cells treated with paraquat displayed substantially large autophagosomes, many of them enclosing mitochondria, which correlates with an increase of p62, an essential mitophagy regulator. Interestingly, autophagy stimulation with rapamycin previous to paraquat treatment prevented these ultrastructural changes. Impairment of motor and cognitive functions induced by paraquat in vivo showed an improvement when autophagy was pre-stimulated. More importantly, dopaminergic neuronal death mediated by paraquat exposure was significantly reduced by rapamycin-induced autophagy in the animal model. Moreover, paraquat-induced microglial activation was diminished by autophagy. Our results suggest that autophagy stimulation might have a protective effect on dopaminergic cells in PD.

Results

Calpain-Dependent and Independent Apoptosis Induced by Paraquat Decreases in Response to Stimulation of Autophagy

Phosphorylation of mTOR plays an essential role in the negative regulation of autophagy [36]. Rapamycin is a well-known autophagy inducer by blocking phosphorylation of mTOR [36, 37]. We validated the rapamycin effect by detecting a decrease of mTOR phosphorylation (Supplementary Fig. S1; Online Resource 1). Then, we corroborated the protective effect of autophagy on the toxicity mediated by paraquat, by exposing dopaminergic cells to increasing concentrations of the neurotoxin in the absence or presence of rapamycin. After 48 h of treatment, cells were analyzed under a microscope (Supplementary Fig. S2a; Online Resource 1) and by trypan blue assay (Supplementary Fig. S2b; Online Resource 1). Paraquat induced a decrease in cell viability in a dose-dependent manner, which was inhibited by autophagy stimulation. Notably, paraquat at 0.5 mM decreased viability to 50%, while autophagy stimulation decreased paraquat toxicity by increasing viability to 72%. This concentration of paraquat was selected for further experiments in vitro.

Cell death induced by paraquat is mediated by caspases (cysteine aspartyl-specific proteases) [28, 29, 38, 39] and calpains (calcium-activated [papain-like] neutral protease) [39, 40], and can be prevented by stimulation of autophagy with rapamycin [28]. Then, we wanted to test whether autophagy stimulation can prevent apoptosis induced by paraquat. Apoptosis was evaluated by detection of phosphatidylserine translocation from the inner to the outer membrane, which is mediated by the scramblase Xrp8 activated by caspase-3 and caspase-7 in early stages of apoptosis [41–43]. Labeling with 7-AAD indicated a loss of plasma membrane integrity. Paraquat increased cell death in a dose-dependent manner, which was significantly decreased when autophagy was stimulated (Fig. 1a, b, representative density plots and bar graph from at least three independent experiments).

We further examined whether autophagy stimulation can prevent calpain-dependent apoptosis induced by paraquat. Endogenous calpain activity was assessed by detecting cleavage of calpain substrate Ac-LLY-AFC at 48 h after treatments. Active calpain was used as positive control and emitted

514 RFU, while calpain Z-LL-FMK inhibitor decreased it to 216 RFU (Fig. 1c). Untreated and rapamycin-treated cells showed values of 230 and 241 RFU, respectively, corresponding to basal levels of calpain activity. Paraquat treatment increased these levels to 373 RFU, and autophagy inducer reduced these levels to 255 RFU. We demonstrated that autophagy exerts a protective effect on calpain-dependent and independent apoptosis induced by paraquat.

Oxidative Stress Induced by Paraquat Decreases in Response to Stimulation of Autophagy

Paraquat induces mitochondrial dysfunction, oxidative stress, autophagy disruption, and cell death [27–30]. Additionally, autophagy downregulation increases oxidative stress in response to nutrients depletion [35]. Therefore, we wanted to test whether autophagy stimulation can decrease oxidative stress induced by paraquat. Dopaminergic cells were exposed to hydrogen peroxide (H_2O_2) for 30 min as a positive control of oxidative stress (Fig. 2a, b). Autophagy was induced by rapamycin previous to exposure to paraquat, and oxidative stress and cell viability were analyzed at 24 h using DHE and calcein-AM, respectively. Untreated and rapamycin-treated cells showed low levels of oxidative stress, while paraquat induced a significant increase in ROS production (Fig. 2a, b). Interestingly, autophagy stimulation decreased ROS levels induced by paraquat. DHE (Fig. 2b) and calcein (Fig. 2c) fluorescence intensity was quantified. The first showed that paraquat increased ROS levels sixfold, while when autophagy was stimulated previous to paraquat exposure, ROS production was decreased to similar levels of untreated cells (Fig. 2b). Cell viability was not affected at 24 h of treatment (Fig. 2c). Likewise, positive cells for ROS increased to 48% in response to paraquat and decreased to 23% when autophagy was induced before paraquat treatment (Fig. 2d, e).

Among the proteins that are the target of oxidation are the peroxiredoxins (PRXs), which in turn catalyze the reduction of H_2O_2, peroxynitrite (HOONO), and most alkyl hydroperoxides [44–46]. PRXs protein levels increase in response to parkinsonian toxins [47, 48]. Oxidative modification of PRX1 occurs in response to the parkinsonian neurotoxin 6-hydroxydopamine, and this effect is inhibited by the antioxidant N-acetylcysteine [48]. Importantly, paraquat has shown to induce oxidation of PRX1 and PRX3 [49]. To determine the effect of paraquat-induced oxidative stress on antioxidant proteins, the oxidative status of PRXs was evaluated. PRXs hyperoxidation was detected by fluorescence microscopy with a specific antibody that recognizes the sulfonylated form of PRXs ($PrxSO_3$) 1 to 4 [50]. We observed that H_2O_2 induced the hyperoxidation of these enzymes (Fig. 3a). Cells treated in the absence or presence of rapamycin showed low levels of PRXs sulfonylation, representing the basal oxidative status of these cells. In contrast, paraquat induced a significant increase of PRXs hyperoxidation (Fig. 3a), and when autophagy was induced before paraquat treatment, this effect was decreased. Fluorescence intensity of PRXs sulfonylation was quantified (Fig. 3b) and showed an increase of fivefold induced by paraquat in comparison with the basal levels of control and rapamycin treatments, while stimulation of autophagy reduced PRXs sulfonylation fluorescence intensity to twofold. These results were confirmed by western blot (Fig. 3c), where both H_2O_2 and paraquat induced a noticeable increase of sulfonylated PRXs, and rapamycin-induced autophagy inhibited the effect produced by paraquat.

Taken together, these results indicate that stimulation of autophagy with rapamycin significantly decreases oxidative stress induced by paraquat.

Autophagy Stimulation Avoids Autophagosome Morphological Changes Induced by Paraquat

Given autophagy inhibition in response to paraquat [28], and considering that oxidative stress is evident at 24 h of treatment, we examined the morphological changes induced by paraquat in dopaminergic cells and determined whether autophagy induction prevents ultrastructural changes. To accomplish this, we used transmission electron microscopy (TEM), the gold standard method to evaluate autophagy [51, 52]. As a result, the typical morphology of dopaminergic cells SH-SY5Y is shown (control) in Fig. 4a. Rapamycin was used as a positive control of autophagy induction, indicating an increased presence of autophagosomes. Surprisingly, paraquat substantially increased the size of autophagosomes (Fig. 4a), and many of them were enclosing mitochondria (mitophagy). Interestingly, when autophagy was stimulated with rapamycin previous to paraquat treatment, autophagosomes size was similar to that observed in control cells. To confirm these findings, cells were analyzed in the presence of the lysosomotropic agent chloroquine, which blocks autophagic flux through inhibition of the autolysosome content, with subsequent autolysosomes accumulation [53, 54]. Chloroquine (40 μM) was added 4 h before harvesting cells. Therefore, chloroquine-treated cells showed more autophagosomes than control cells, indicating blockage of basal autophagic flux. Rapamycin-treated cells in the presence of chloroquine showed an increased number of autophagosomes compared with chloroquine alone. Unexpectedly, enlarged autophagosomes found in paraquat-treated cells were not present when co-treated with chloroquine, and cell morphology was similar to that of chloroquine-treated cells. Besides, the morphology of cells co-treated with rapamycin and paraquat in the presence of chloroquine resembles that of chloroquine-treated cells too, which indicates that rapamycin-induced autophagy was indeed able to prevent morphological changes produced by paraquat.

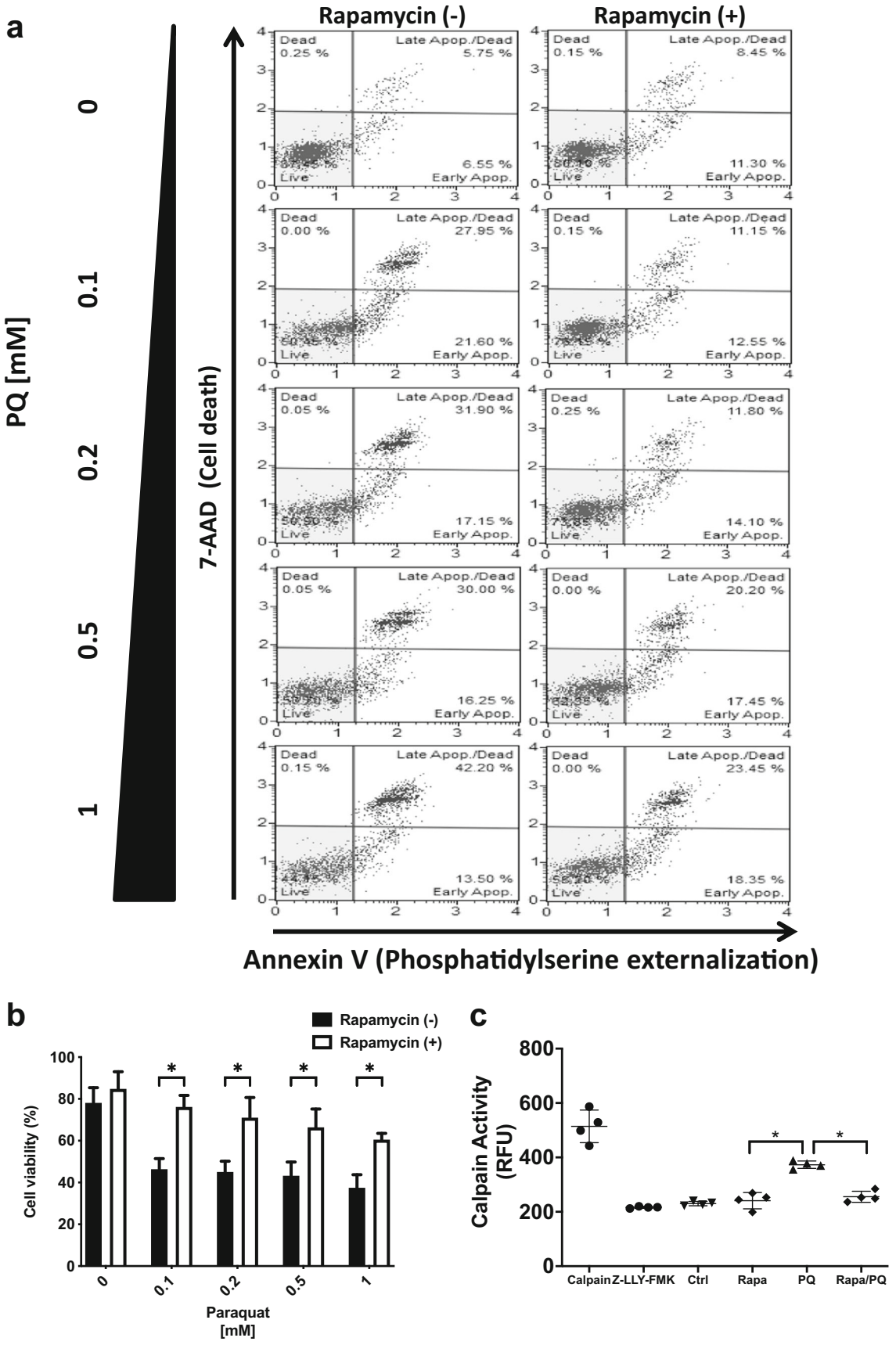
a
Rapamycin (-)
Rapamycin (+)
PQ [mM]
0
0.1
0.2
0.5
1
7-AAD (Cell death)
Annexin V (Phosphatidylserine externalization)
Dead 0.25 % Late Apop./Dead 5.75 % Live 6.55 % Early Apop.
Dead 0.15 % Late Apop./Dead 8.45 % Live 11.30 % Early Apop.
Dead 0.00 % Late Apop./Dead 27.95 % Live 21.60 % Early Apop.
Dead 0.15 % Late Apop./Dead 11.15 % Live 12.55 % Early Apop.
Dead 0.05 % Late Apop./Dead 31.90 % Live 17.15 % Early Apop.
Dead 0.25 % Late Apop./Dead 11.80 % Live 14.10 % Early Apop.
Dead 0.05 % Late Apop./Dead 30.00 % Live 16.25 % Early Apop.
Dead 0.00 % Late Apop./Dead 20.20 % Live 17.45 % Early Apop.
Dead 0.15 % Late Apop./Dead 42.20 % Live 13.50 % Early Apop.
Dead 0.00 % Late Apop./Dead 23.45 % Live 18.35 % Early Apop.
b
Rapamycin (-)
Rapamycin (+)
Cell viability (%)
Paraquat [mM]
c
Calpain Activity (RFU)
Calpain
Z-LLY-FMK
Ctrl
Rapa
PQ
Rapa/PQ

◀ **Fig. 1** Autophagy stimulation decreases calpains-dependent and independent cell death induced by paraquat. **a**, **b** SH-5YSY cells were exposed to different concentration of paraquat (0, 0.1, 0.2, 0.5, and 1 mM) for 48 h. Rapamycin (10 μM) was added 1 h before paraquat treatment. Annexin V-7AAD measured apoptosis through flow cytometry. In dot-plots, early apoptosis is represented as an increase in the number of Annexin V (+)/7AAD (−) cells (lower right quadrant). Late-apoptotic and necrotic cells are identified as Annexin V (+)/7AAD (+) (upper left quadrant). Plots are representative of three independent experiments (plots in **a**, and bar graph in **b**). Apoptotic cell death was induced in a paraquat dose-dependent manner, and rapamycin increased cell viability to counteract cell damage induced by paraquat. **c** Cytosolic proteins from treated-cells (rapamycin 10 μM, paraquat 0.5 mM, or both) were isolated, and cleavage of calpain substrate Ac-LLY-AFC assessed endogenous calpain activity through fluorometry. Active calpain was used as a positive control and the calpain inhibitor Z-LLY-FMK as a negative control. RFU, relative fluorescence units. A probability value of $*p < 0.05$ was considered statistically significant. Ctrl, control; Rapa, rapamycin; PQ, paraquat

Fifty cells per treatment were evaluated by morphometric analysis using TEM to determine the extent of mitophagy in response to paraquat. Untreated and rapamycin-treated cells showed 8 and 16% of mitophagy, respectively (Fig. 4b). In response to paraquat, 34% of cells were positive for mitophagy, while it was reduced to 24% when autophagy was induced before exposure to paraquat. It is worth to notice that paraquat affected the mitochondrial cristae integrity (Fig. 4c), and endoplasmic reticulum isolation membranes (phagophore expansion) were prevalent surrounding damaged mitochondria.

These results were confirmed by western blot (Fig. 4d), where LC3-II, the hallmark of autophagy was evaluated. LC3-II was increased in response to rapamycin and decreased in response to paraquat. Differences between treatments in the presence of chloroquine were consistent with the observed by TEM.

Since the presence of damaged mitochondria enclosed by autophagosomes was evident in response to paraquat, we evaluated p62, an essential mitophagy regulator that mediates the aggregation of damaged mitochondria [55]. As a result, paraquat induced a noticeable increase of p62, which was decreased when autophagy was stimulated before paraquat treatment (Fig. 4e). In the presence of Mito Tracker Red CM-H_2XROS, mitochondrial oxidative stress was increased by paraquat and co-localized with p62 when autophagy was induced with rapamycin before paraquat treatment (Supplementary Fig. S3; Online Resource 1), which suggests that oxidative stress-damaged mitochondria are prone to be engulfed by autophagosomes.

Autophagy Stimulation Improves the Motor and Cognitive Functions Impaired by Paraquat

Afterward, we wanted to determine whether the protective effect of autophagy against paraquat toxicity was kept in vivo. Autophagy was stimulated 1 week before paraquat treatment. Mice body weight was recorded once a week throughout treatments, and a non-significant difference between groups was observed (Supplementary Fig. S4; Online Resource 1).

Since the loss of motor coordination is one of the main characteristics of PD [56–58], we determined whether paraquat-induced PD model showed motor alterations, as previously reported [59]. The control group showed normal posture and movement (Fig. 5a). Motor abilities of the rapamycin-treated group were similar to the control group. However, mice treated with paraquat showed a slightly flexed posture at rest and raised their hind legs noticeably during walking, which indicates that motor function was significantly affected compared to the control group. Furthermore, mice co-treated with rapamycin and paraquat displayed a slight but not statistically different recovery in posture and movement compared to those that only received paraquat (Fig. 5a).

Cognitive dysfunction is a non-motor symptom of PD patients [56]. This feature was assessed in mice based on their nest-building ability, which is sensitive to brain injury [60], engages orofacial and forelimb movement, and is dopamine-dependent [59]. Since mice instinctively build nests, a disorganized nest might evidence either cognitive or motor dysfunction [59–61]. Both control and rapamycin group constructed a well-organized complete dome-shaped nest (Fig. 5b, c). However, mice behavior was affected by paraquat, which was evidenced by a disorganized cup-shaped nest building. Unexpectedly, autophagy induction with rapamycin restored the nest building ability of mice affected by paraquat (Fig. 5b, c).

Induction of Autophagy Decreases the Loss of Dopaminergic Neurons Mediated by Paraquat

Next, we sought to investigate whether the improvement induced by autophagy on the motor and cognitive functions impaired by paraquat was related to a protective effect in dopaminergic neurons. Midbrain dopaminergic neurons were examined. Figure 6a shows the average population of dopaminergic neurons from the control group, which was not affected by rapamycin. In contrast, the group treated with paraquat exhibited a noticeable decrease in dopaminergic neurons compared to the control group. Interestingly, autophagy stimulation decreased dopaminergic neuronal loss induced by paraquat. These results were corroborated by tyrosine hydroxylase (TH) positive neurons count (Fig. 6b).

Additionally, these results were confirmed by western blot (Fig. 6c), where paraquat induced a significant decrease in TH protein levels and autophagy stimulation before paraquat treatment increased TH protein levels. Besides, we showed that paraquat decreased LC3-II protein levels in vivo. Surprisingly, induction of autophagy preceding paraquat treatment led to similar LC3-II protein levels than those observed

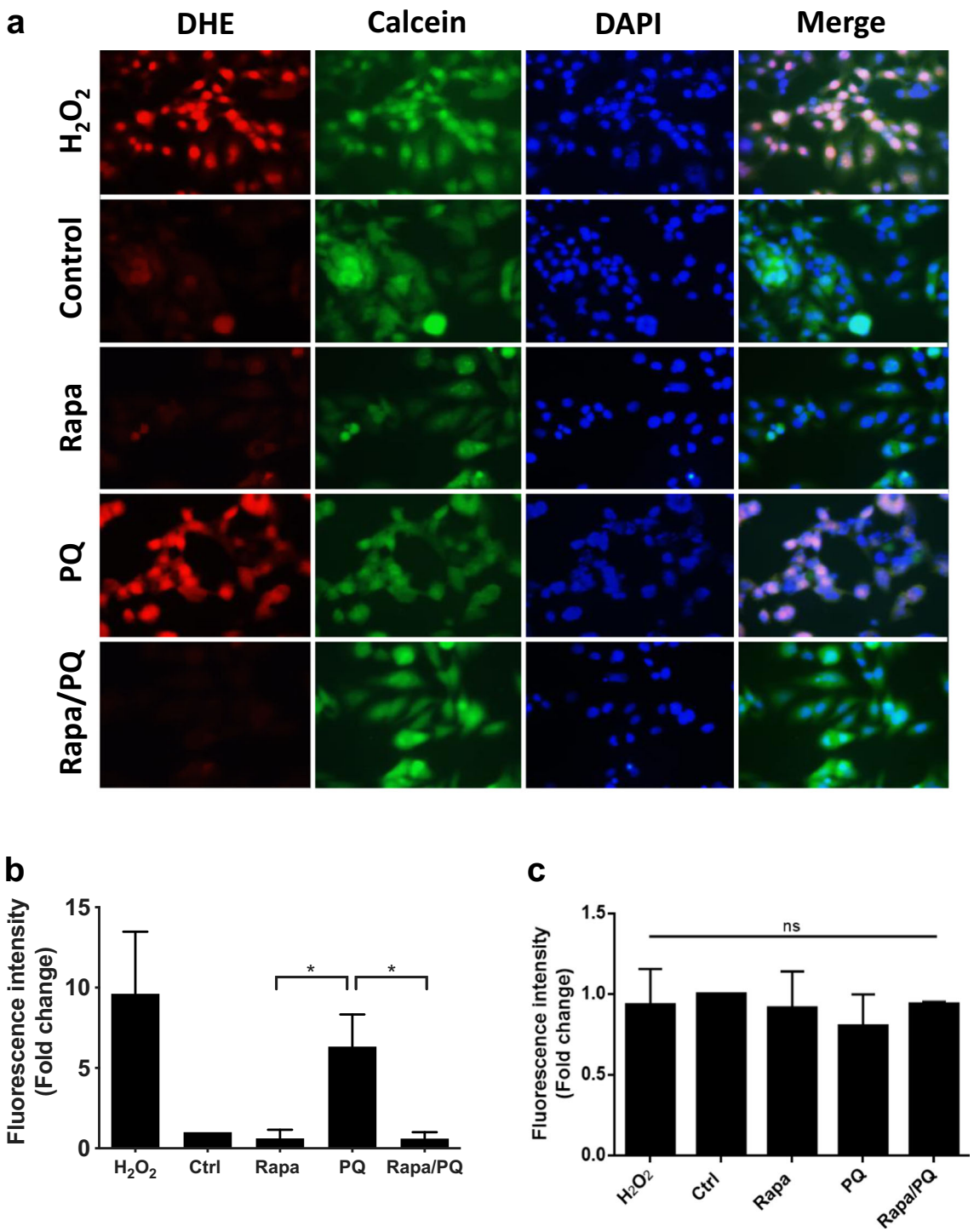

Fig. 2 Oxidative stress induced by paraquat decreases upon autophagy stimulation. SH-SY5Y cells were pre-treated with the inducer of autophagy rapamycin (10 μM) 1 h before paraquat (0.5 mM) was added, and cells were analyzed 24 h after treatment. Hydrogen peroxide (H_2O_2, 20 mM for 30 min) was used as positive control of oxidative stress. **a** Fluorescence micrographs show the cytoplasmic oxidative stress detected with DHE (5 μM, red fluorescence), cell viability detected with calcein (5 μM, green fluorescence), and nuclear staining with DAPI (blue fluorescence). **b** Statistical analysis of the fluorescence intensity of DHE, which shows an increase in response to paraquat and a decrease when autophagy is induced before paraquat treatment. **c** Statistical analysis of the fluorescence intensity of calcein, showing that viability is not affected at 24 h by the treatments. **d** Flow cytometry analysis of treated cells stained with DHE. Histograms are representative of 3 independent experiments. **e** Statistical analysis of (**d**). A probability value of $*p < 0.05$ was considered statistically significant. Ctrl, control; Rapa, rapamycin; PQ, paraquat; ns, not significant

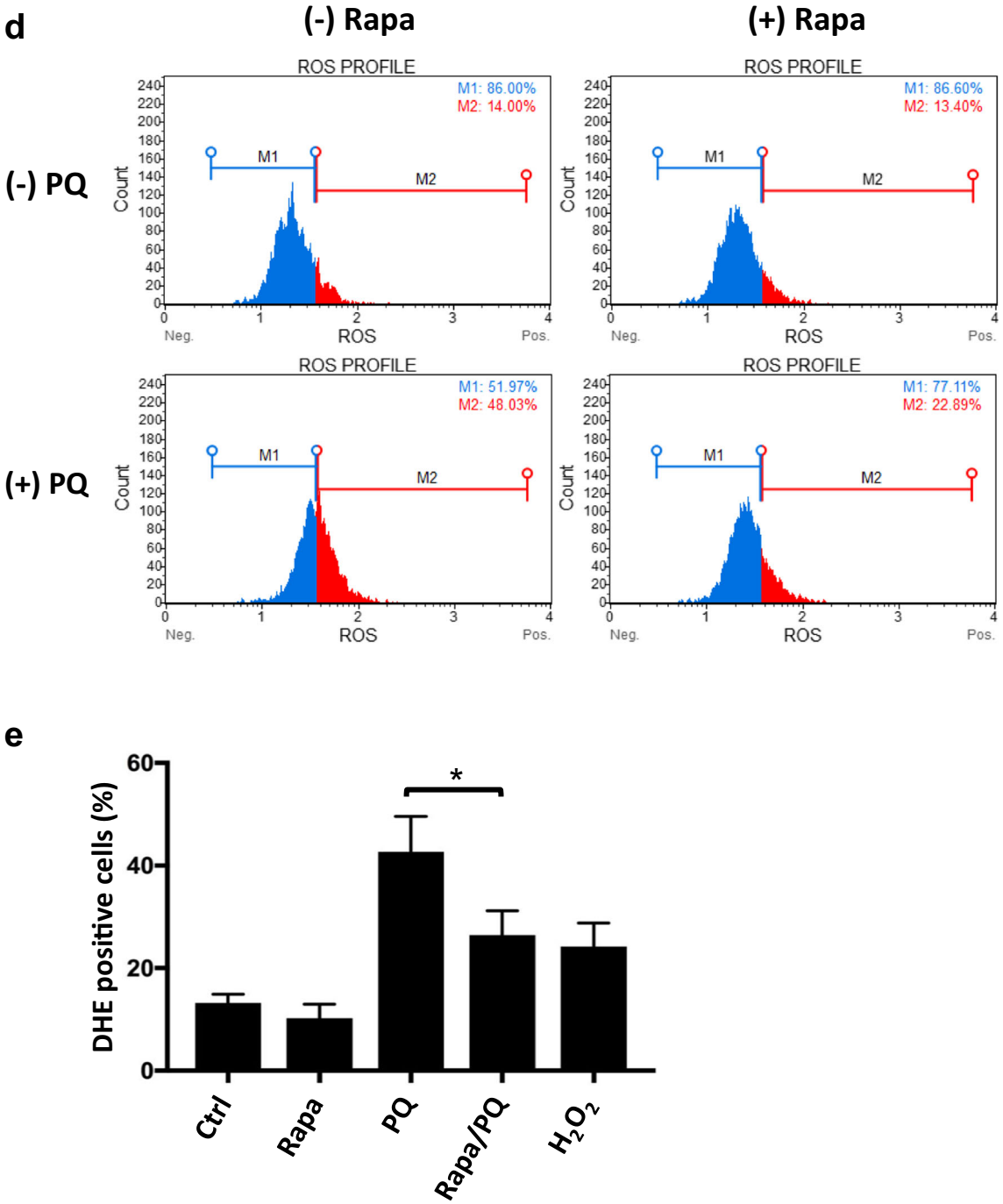

Fig. 2 (continued)

in the control group. Therefore, we demonstrated that rapamycin-stimulated autophagy inhibits dopaminergic neuronal death induced by paraquat.

Induction of Autophagy Decreases Paraquat-Induced Microglial Activation

Microglial activation in postmortem brain samples of PD patients [62] suggests that both microglial activation and inflammation play an essential role in the pathogenesis of PD. Because paraquat induces microglial activation [63, 64], we aim to determine the effect of autophagy on its activation. Low levels of microglial activation were observed in both control and rapamycin groups (Fig. 7a). Conversely, paraquat induced a dramatic increase in microglial activation, while a remarkable decrease was detected when autophagy was stimulated before paraquat treatment. To validate these results, IBA-1 positive cell count was performed and showed an evident increase of these cells in response to paraquat treatment, whereas autophagy induction with rapamycin significantly reduced the microglia activated by paraquat (Fig. 7b).

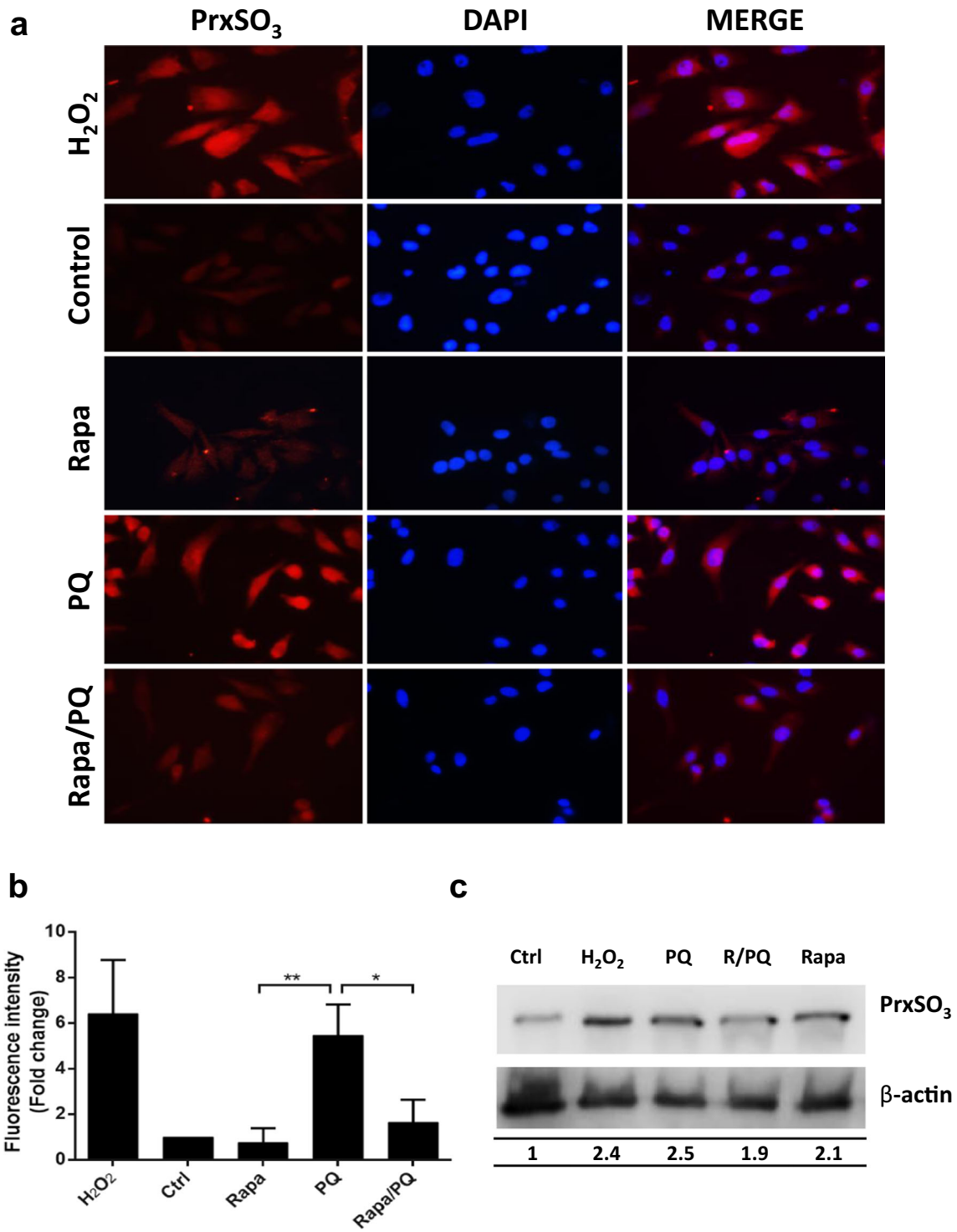

Fig. 3 Effect of autophagy on peroxiredoxins (PRXs) oxidative status induced by paraquat. SH-SY5Y cells were pre-treated with rapamycin 1 h before paraquat was added. Cells were analyzed 24 h after treatment with a specific anti-$PrxSO_3$ antibody by **a** immunofluorescence, where nuclear staining with DAPI is showed; and by **c** western blot, where β-actin was used as a loading control. Densitometry values are indicated below each lane and were normalized to β-actin. **b** Statistical analysis of the fluorescence intensity of (**a**), where a probability value of $*p < 0.05$ was considered statistically significant. Note the strong induction of PRXs hyperoxidation in response to paraquat, and how this is prevented when autophagy is stimulated. Ctrl, control; Rapa, rapamycin; PQ, paraquat

Discussion

Prevention and treatment of PD are still deficient and limited. Because human lifespan has steadily increased since the nineteenth century [65], neurodegenerative diseases including PD are becoming more prevalent. Therefore, the development of preventive and prophylactic treatments to counter PD is essential. Among potential mechanisms to be explored as therapeutics, regulation of autophagy is quite promising as strong evidence indicates that autophagy dysfunction leads to neurodegeneration [21–24].

As oxidative stress characterizes paraquat-induced PD model, and autophagy impairment enhanced the toxicity mediated by paraquat, whereas its stimulation reduced this effect in vitro [27–30], we investigated the hypothesis that autophagy stimulation decreases apoptotic cell death by reducing oxidative stress. We have previously seen that oxidative stress initiates in mitochondria and spreads into the cytoplasm, preceding cell death in response to paraquat [27]. Besides, exposure to paraquat leads to protein oxidation and lipid peroxidation [27].

Herein, we demonstrated that stimulation of autophagy with rapamycin exerts a protective effect on both calpain-dependent and independent apoptosis induced by paraquat. These results correlate with a study where rapamycin prevented caspase-3 activation mediated by MPP^+ [66]. Rapamycin also protected both SH-SY5Y cells and primary mesencephalic cell cultures against rotenone-induced dopaminergic cell death [67, 68]. Likewise, calpains involvement in the dopaminergic neuronal death in PD has been previously established [69, 70]. Calpains inhibition attenuated MPTP adverse effects on dopaminergic neurons and locomotor function [70]. Those results correlate with our findings in vitro, where calpain-mediated cell death induced by paraquat was indeed decreased by autophagy stimulation, and in vivo, where the motor dysfunction we observed in the PD animal model was also reduced. Also, calcium may be released into the cytoplasm as a result of an enduring mitochondrial dysfunction [66, 69, 71, 72], as observed in PD and the response to paraquat, with the subsequent calpain activation.

Moreover, we determined that indeed autophagy induction decreased both oxidative stress and PRXs hyperoxidation induced by paraquat. Our results are consistent with a study where knockdown of autophagy-related genes *ATG5* and *ATG10* increased ROS induced by starvation [35], suggesting a protective role of autophagy against oxidative stress. Another study showed that autophagy induced with rapamycin decreased the levels of the lipid peroxidation biomarker malondialdehyde (MDA) in a PD animal model induced with 6-hydroxydopamine (6-OHDA) [73]. Besides, rapamycin was also able to decrease oxidative heart stress in vivo [74].

Because oxidative stress is quite evident in response to paraquat, we infer cellular morphological changes could accompany it. The gold standard method to demonstrate autophagosomes, lysosomes, and autolysosomes presence is TEM [51, 52]. However, dynamic turnover cannot be quantified unless a time-point analysis is performed [52]. To evidence a clear autophagy regulation can be difficult, to some extent, because of the rapid turnover of intermediary autophagic structures. As previously reported [75], we observed the presence of mitophagy in response to paraquat, with extremely large autophagosomes. These events, where mitochondria are targeted for clearance by the autophagic machinery, may be related to oxidative damage within mitochondria [27], in an attempt to avoid further irreversible oxidative modifications and damage. However, we have seen that this cellular response is not enough to prevent cell death induced by paraquat. Interestingly, when autophagy was stimulated with rapamycin previous to paraquat treatment, autophagosome size was similar to that of control cells, and mitophagy was not observed.

Moreover, these results were confirmed when autophagic flux was blocked with chloroquine. In this regard, the expected accumulation of enlarged autophagosomes found in paraquat-treated cells was not observed when autophagic flux was inhibited with chloroquine, and cells' morphology was similar to that of cells treated with chloroquine alone. These results are consistent with a previous report of impairment of autophagic flux by paraquat [28]. Even though chloroquine-expected effect in paraquat-treated cells was not observed, results were intriguing and leave an open question about the interaction these drugs may have. However, the morphology of cells co-treated with rapamycin and paraquat in the presence of chloroquine was similar to that of chloroquine-treated cells too, which indicates that rapamycin-induced autophagy was indeed able to prevent morphological changes produced by paraquat.

After that, we wanted to determine whether the protective effect of autophagy against paraquat toxicity was preserved in vivo. Previously, it has been reported that paraquat produces a decline in motor function [76]. Another research found a significant deficiency in nest building behavior in a PD animal model induced with MPTP [59]. Our study shows not only motor but a cognitive disruption in response to paraquat. Foremost, we observed that impairment of motor and cognitive functions induced by paraquat showed an improvement when autophagy was pre-stimulated with rapamycin, suggesting a protective role of autophagy. These results agree with the prophylactic effect of rapamycin observed on the cognitive deficit in an Alzheimer's disease model [77].

Because paraquat preferentially decreases nigrostriatal dopaminergic neurons [78–80], we aimed to determine whether autophagy stimulation with rapamycin can prevent this effect. Importantly, the present work shows that rapamycin-induced autophagy significantly reduced dopaminergic neuronal death mediated by paraquat exposure in vivo. Our results are consistent with the

protective effect of rapamycin against the toxicity induced by other parkinsonian toxins suchlike MPTP and 6-OHDA [73, 81, 82].

Nonetheless, microglia play a pivotal role in neuronal maintenance, representing 10% of all glial cells [62]. Microglial activation has been reported in postmortem brain samples of PD patients [62], indicating that neuroinflammation plays an essential role in the pathogenesis of PD. Experimental animal models using different species that were exposed to MPTP, 6-OHDA, or rotenone displayed activated microglia in the *substantia nigra* [83–88]. Additionally, microglial activation has also been reported in response to paraquat [63, 64]. Therefore, we sought to explore the effect of autophagy stimulation on paraquat-induced microglial activation in vivo. Interestingly, paraquat-induced microglial activation was diminished by the stimulation of autophagy with rapamycin. These results are consistent with a recent study where autophagy induced by metformin inhibited microglial activation in the MPTP plus probenecid PD model [89].

In summary, our findings suggest an interplay between autophagy and oxidative stress, where either autophagy disruption or excessive oxidative stress is detrimental for neurons, while autophagy stimulation can decrease oxidative stress, mitophagy, and calpain-dependent and independent apoptosis induced by paraquat in vitro. Also, autophagy protective effect was demonstrated in vivo by reducing dopaminergic neuronal loss and microglial activation, which explained the motor and cognitive improvement in mice compared with paraquat treatment by itself. Therefore, autophagy inducers may be suitable candidates for the treatment of neurodegenerative diseases. More research in the mechanistic interrelation between autophagy and redox signaling is essential to shed light on the challenges of development of neuroprotective therapeutics.

Materials and Methods

Cell Culture and Reagents

Human dopaminergic neuroblastoma cell line SH-SH5Y was obtained from the American Type Culture Collection (#CRL-2266, ATCC, Manassas, VA). Cells were cultured in DMEM/F12 medium (#11330-032, Thermo Fisher Scientific, Waltham, MA) containing 10% heat-inactivated fetal bovine serum (#35-010-cv, Thermo Fisher Scientific), 100 units/ml penicillin-streptomycin (#30-004-Cl, Corning) in a humidified 37 °C incubator with 5% CO_2. Cells were treated with paraquat (1,1′-dimethyl-4,4′-bipyridinium dichloride) at 0.1–1 mM (#AC227320010, Thermo Fisher Scientific or #36541, Millipore Sigma, St. Louis, MO) for 24 h (oxidative stress assays) or 48 h (cell death assays). Rapamycin (#R-5000, LC Laboratories, Woburn, MA) was used to stimulate autophagy, at a final concentration of 10 μM, 1 h before paraquat treatment.

Fig. 4 Autophagy stimulation prevents morphological alterations induced by paraquat. SH-SY5Y cells were pre-treated with rapamycin 1 h before treatment with paraquat and incubated for an additional 24 h. Autophagic flux was blocked with chloroquine (CQ, 40 μM), which was added 4 h before fixing and harvesting cells for their further analysis by **a** transmission electron microscopy. Representative electron micrographs are showed. **b** Mitophagy (autophagosomes enclosing mitochondria) was evaluated by morphometric analysis using TEM, where 50 cells per treatment were analyzed. Results are expressed as a percentage of mitophagy. **c** Paraquat-treated cells show disruption of mitochondrial cristae (dotted arrows) and phagophore expansion (arrows) is in close proximity to damaged mitochondria. Boxed areas are enlarged in the right column. Ultrastructural changes related to autophagy (autophagosomes) were correlated with **d** the autophagy marker LC3-II and **e** the mitophagy marker p62 by western blot, where GAPDH or β-actin were used as a loading control. Densitometry values were normalized to GAPDH or β-actin from three independent experiments. A probability value of $*p < 0.05$ was considered statistically significant. Rapa, rapamycin; PQ, paraquat; nucleus (N); mitochondrion (m); lipid inclusion (L); lysosome (Ly); an asterisk (*) indicates autophagosomes

Apoptosis Assay

Apoptosis was determined by using the Muse Annexin V & Dead Cell Kit (#MCH100105, Millipore Sigma). This assay relies on the ability of Annexin V to bind to phosphatidylserine, a marker of apoptosis, and the uptake of 7-amino actinomycin D (7-AAD) as a marker for loss of plasma membrane integrity. Data are represented as a percentage of viability. Early apoptotic cells are defined as having Annexin V-positive and 7-AAD-negative staining. Late-apoptotic and nonviable cells are both Annexin V and 7-AAD positive.

Calpain Activity Assay

Endogenous calpain activity was measured with the Calpain Activity Assay Kit (#ab64380, Abcam, Cambridge, MA). Briefly, after treatments, cytosolic proteins were isolated with an extraction buffer. Calpain substrate Ac-LLY-AFC was added; upon cleavage of the substrate by calpain, free AFC emits a yellow-green fluorescence (λ max = 505 nm), which was quantified using a microplate fluorescence reader (FLx800TB, BioTek Instruments, Winooski, VT). Results are expressed as relative fluorescence units (RFU). Active calpain was used as positive control and the calpain inhibitor Z-LLY-FMK as a negative control.

Oxidative Stress Detection

Cells were incubated with dihydroethidium (DHE, #D11347, Thermo Fisher Scientific) at 5 μM for 15 min (ex. 490, em. 570 nm), or Mito Tracker Red

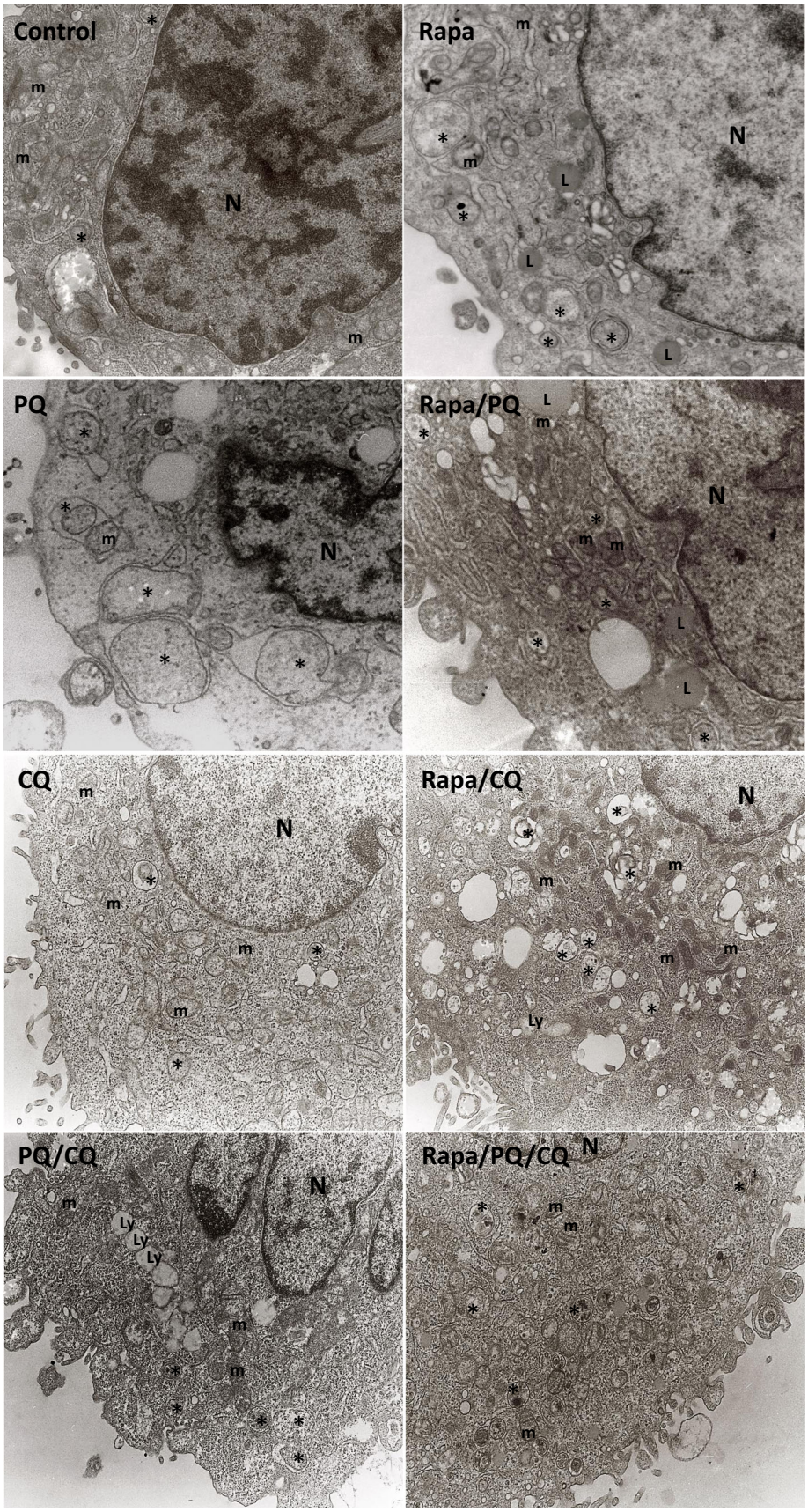
a
Control
Rapa
PQ
Rapa/PQ
CQ
Rapa/CQ
PQ/CQ
Rapa/PQ/CQ
N
m
L
Ly

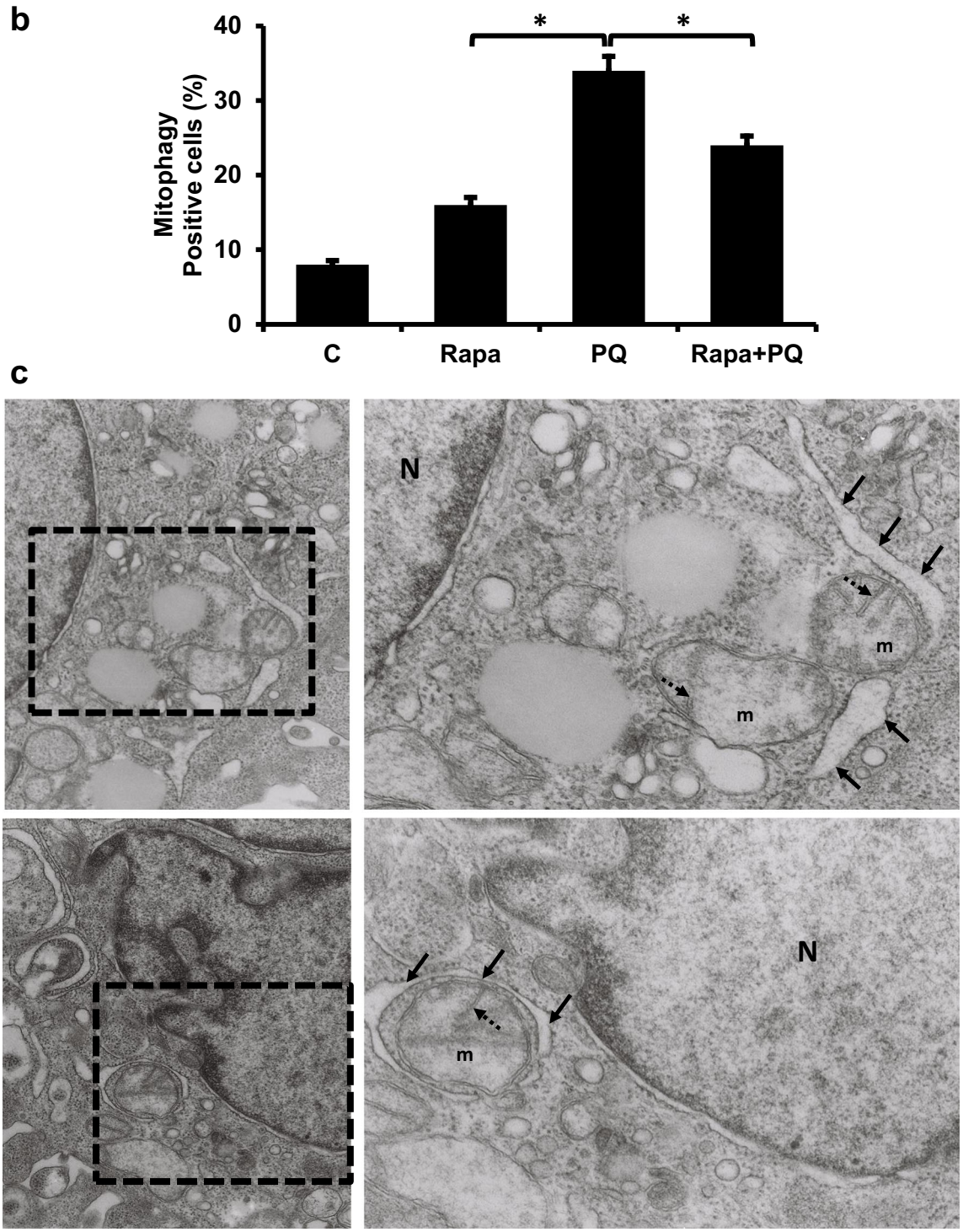

Fig. 4 (continued)

CM-H_2XROS (#M7513, Thermo Fisher Scientific) at 500 nM for 1 h (ex. 580, em. 600), and its oxidation was monitored by fluorescence microscopy. Nuclei were stained with VECTASHIELD Antifade Mounting Medium with DAPI (#H1200, Thermo Fisher Scientific). Cell survival was assessed using a calcein retention assay, which measures cell viability. Cells were incubated with calcein-AM (#354217, Thermo Fisher Scientific) at 5 μM (ex. 485, em. 530 nm) for 15 min. Then, cells were washed and analyzed in a Nikon Eclipse 50i fluorescent microscope (Nikon, Melville, NY). Fluorescence intensity was quantified using ImageJ (NIH) v3.91 software (http://rsb.info.nih.gov/ij). Alternatively, treated cells were incubated with

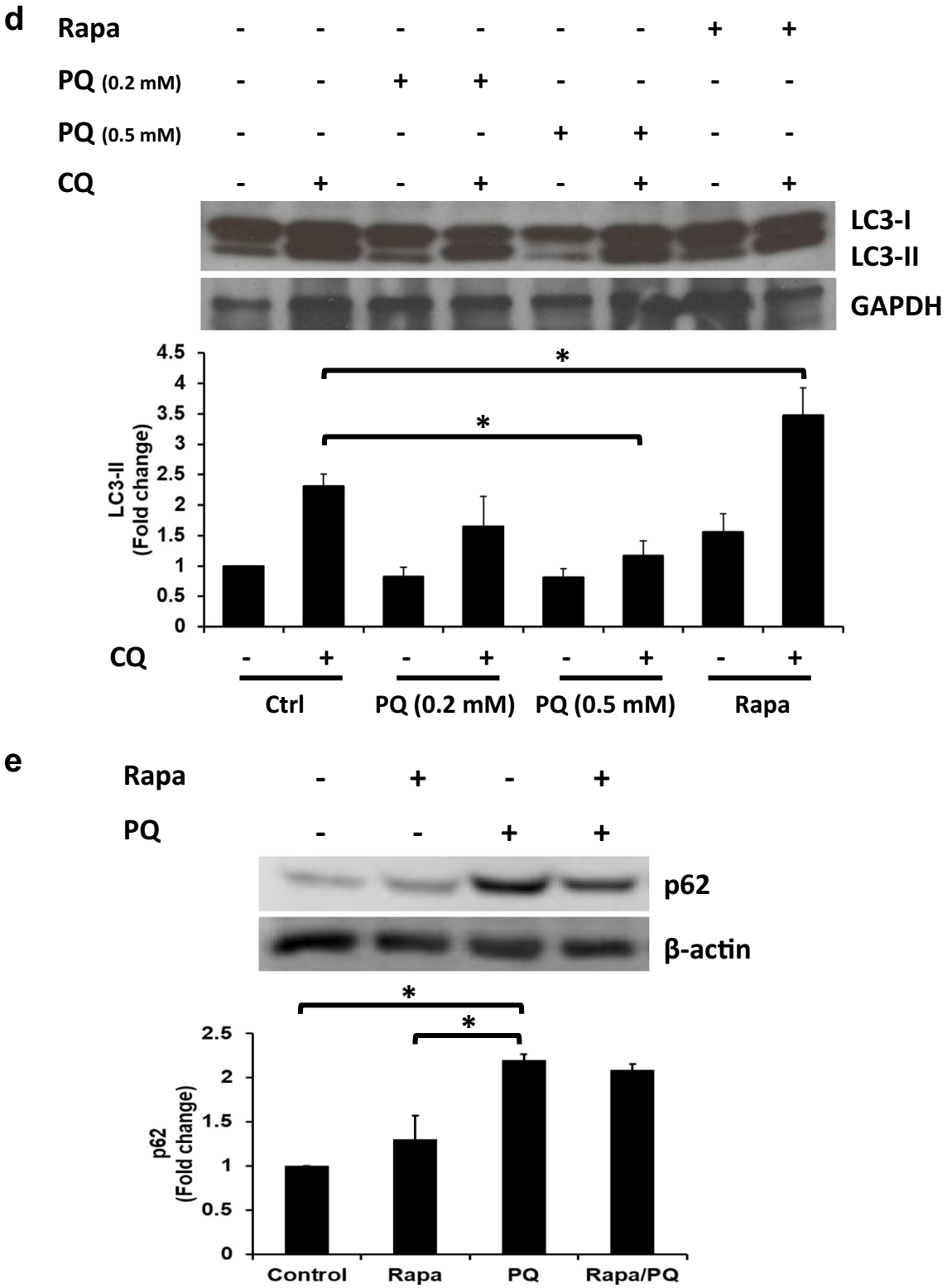

Fig. 4 (continued)

DHE (10 μM) for 15 min, harvested with trypsin, and resuspended in PBS 1x. Finally, cells were evaluated by flow cytometry (Muse Cell Analyzer, Millipore Sigma).

Western Immunoblotting (WB)

Cells or midbrain samples were lysed in radioimmunoprecipitation assay (RIPA) buffer (20 mM Tris-

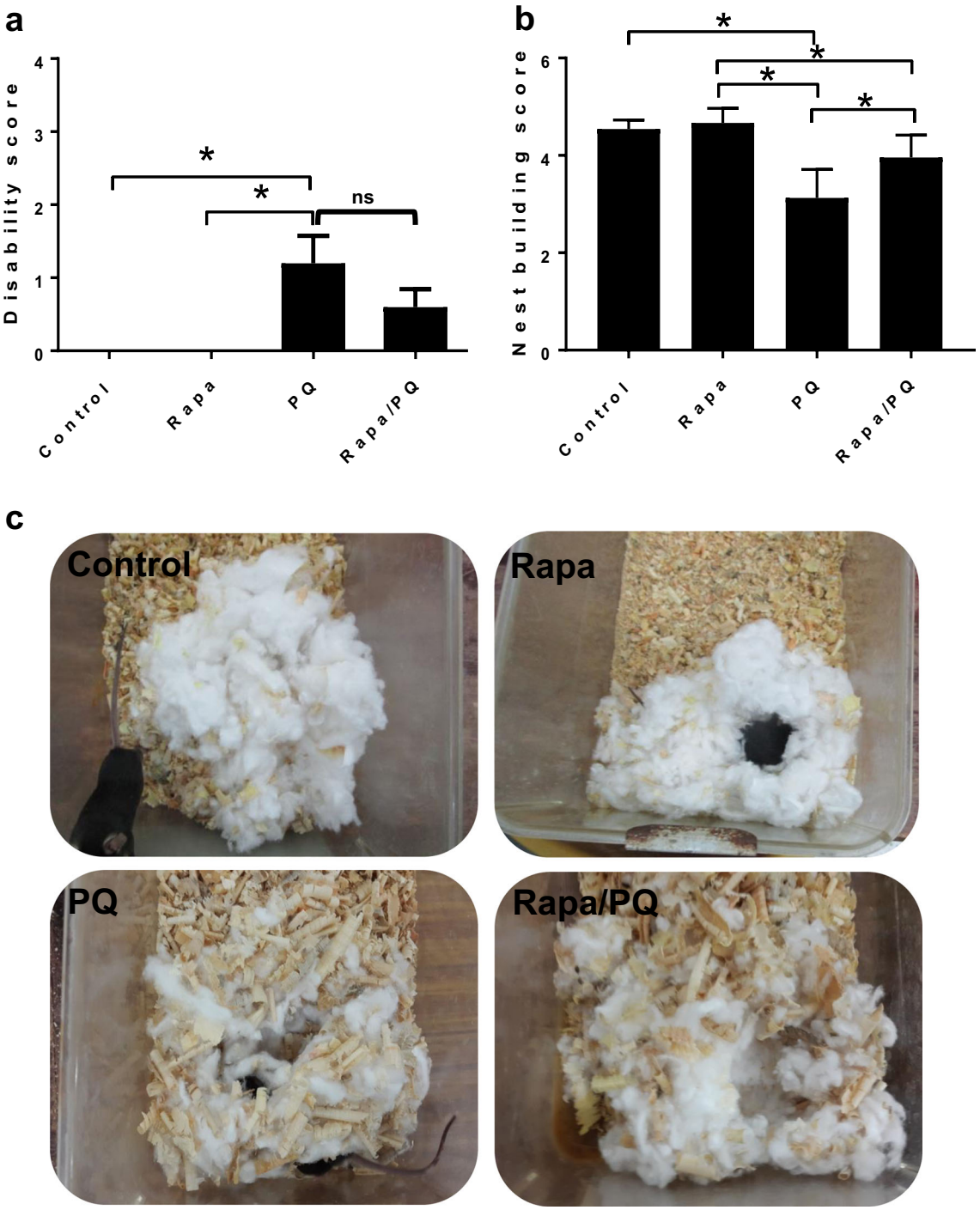

Fig. 5 Motor and behavioral disabilities induced by paraquat decrease upon autophagy stimulation. **a** Disability score was assessed individually in all mice at the end of the animal model, as a sum of gait and body posture abnormalities by direct visual inspection in their cages. Note that paraquat affects motor function, while co-treatment with rapamycin and paraquat displayed a slight no statistically significant difference of recovery in posture and movement. **b**, **c** Nests were scored as follows: 5 = complete dome-shaped nest, 4 = incomplete dome-shaped nest, 3 = cup-shaped nest, 2 = flat nest, 1 = disturbed, and 0 undisturbed nesting material. A probability value of $*p < 0.05$ was considered statistically significant. Rapa, rapamycin; PQ, paraquat; ns, not significant

HCl, 150 mM NaCl, 1 mM Na_2EDTA, 1 mM ethylene glycol tetraacetic acid (EGTA), 1% Triton X-100) containing Halt Protease and Phosphatase Inhibitor Cocktail (#78446, Thermo Fisher Scientific). Samples were sonicated and centrifuged, and pellets were discarded. Twenty-five to 50 μg of protein per sample were loaded and separated by SDS-polyacrylamide gel electrophoresis and transferred to PVDF or nitrocellulose membranes. Blots were incubated at

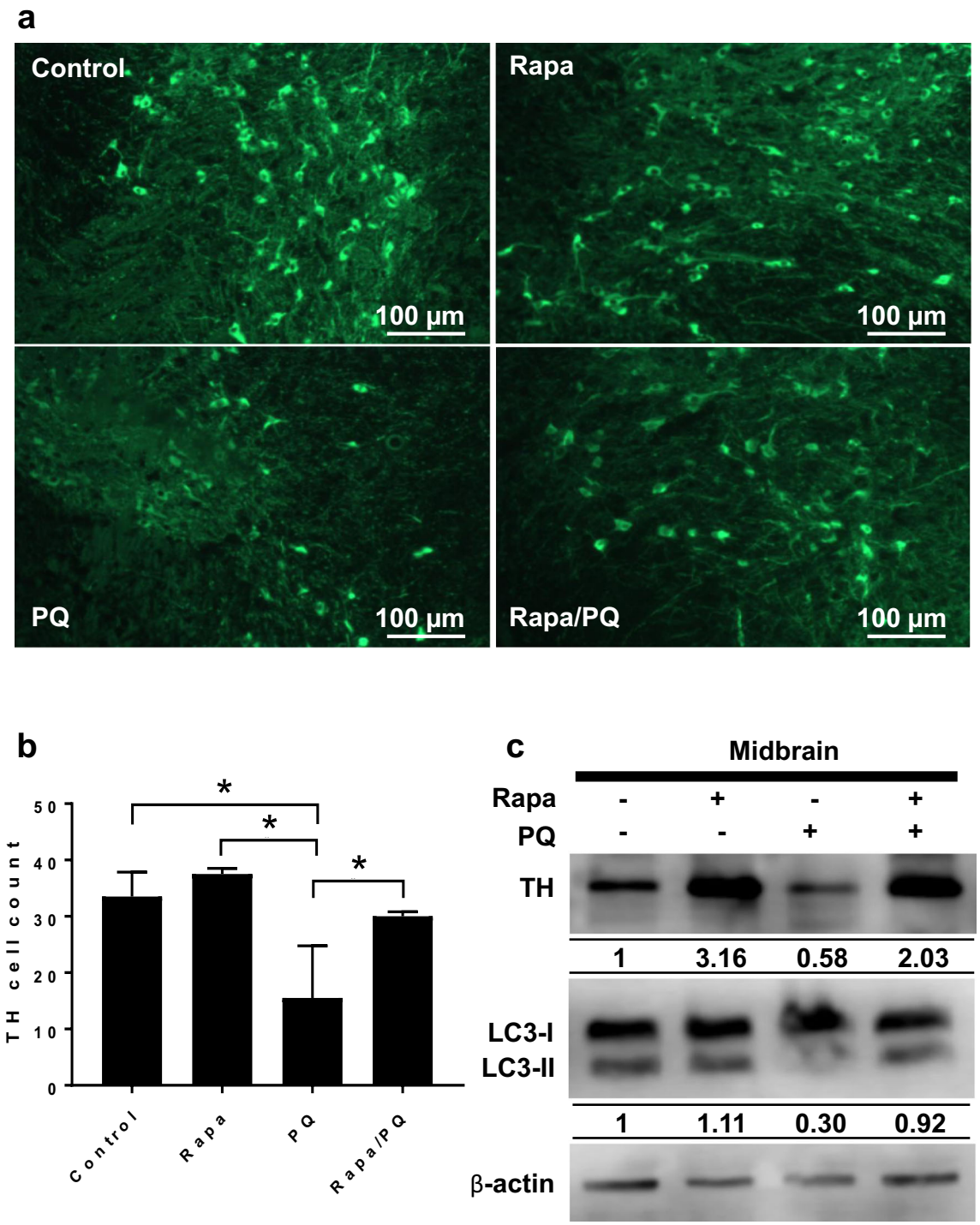

Fig. 6 Autophagy stimulation decreases dopaminergic neuronal death induced by paraquat. **a** Midbrain sections were subjected to immunostaining with anti-TH to detect dopaminergic neurons, which were decreased in response to paraquat, while this effect was prevented when autophagy was induced. **b** TH-positive neurons count was performed in four random fields per section. A probability value of $*p < 0.05$ was considered statistically significant. **c** TH and autophagy marker LC3-II were both decreased by paraquat, which was inhibited by rapamycin-stimulated autophagy. Densitometry values are shown below blots and were normalized to β-actin. Rapa, rapamycin; PQ, paraquat

4 °C overnight with the appropriate primary antibody (1:1000): rabbit anti-mTOR (phospho S2448) (#ab109268, Abcam), rabbit anti-mTOR (#ab2732, Abcam), rabbit anti-$PrxSO_3$ (#ab16830, Abcam) rabbit anti-LC3B (#L7543, Millipore Sigma), rabbit anti-SQSTM1/p62 (#ab155686, Abcam), rabbit anti-TH (tyrosine hydroxylase) (#ab112, Abcam), and rabbit anti-β-actin (#A5060, Millipore Sigma) or rabbit anti-GAPDH (#2118, Cell Signaling Technology,

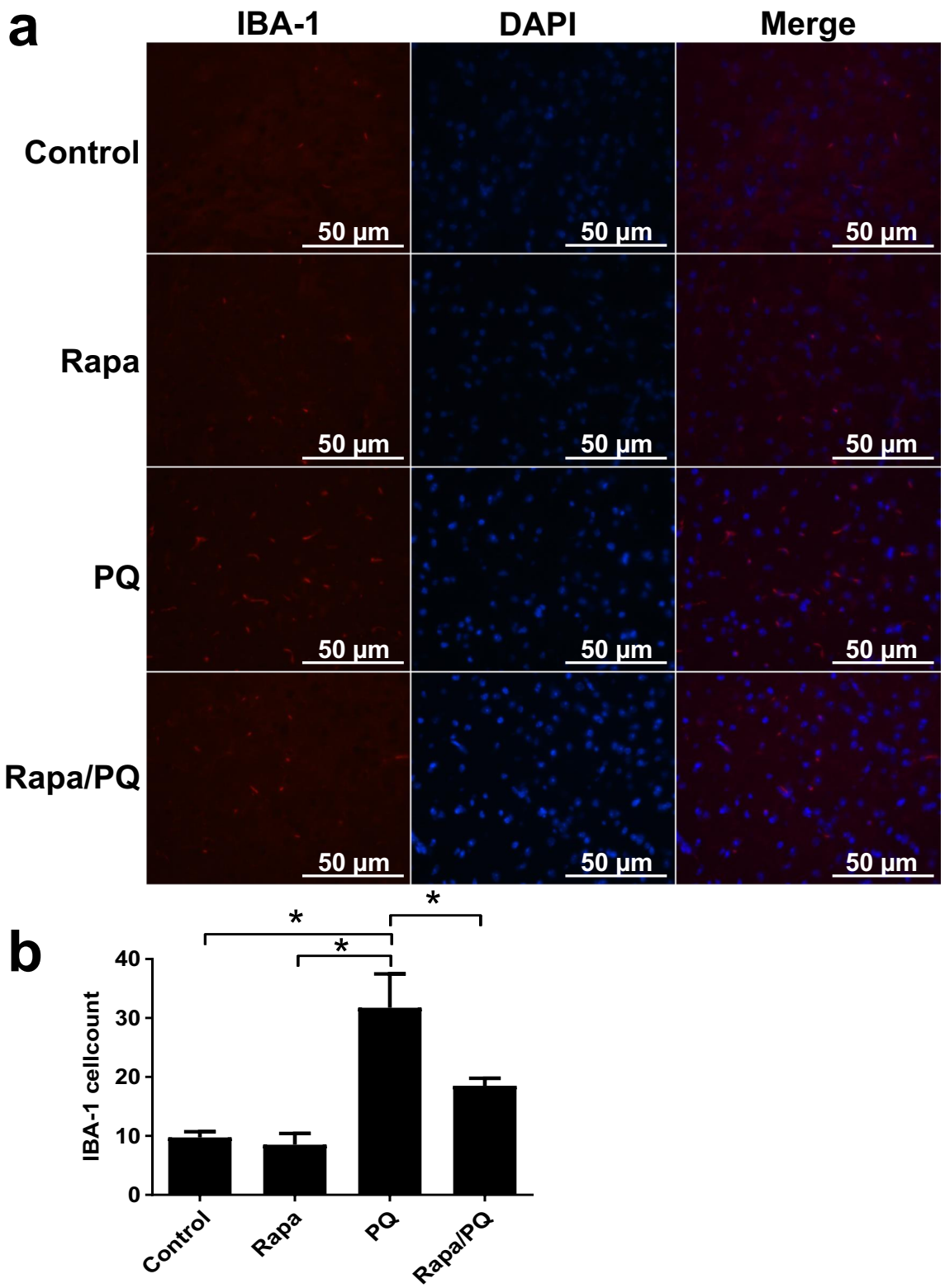

Fig. 7 Autophagy stimulation prevents microglial activation triggered by paraquat. **a** Midbrain sections were incubated with anti-IBA-1. Nuclear staining with DAPI is shown. Notice that paraquat increases microglial activation, while rapamycin inhibits microglial activation induced by paraquat. **b** IBA-1-positive cells count was performed in four random fields per section. A probability value of $*p < 0.05$ was considered statistically significant. Rapa, rapamycin; PQ, paraquat

Danvers, MA), to verify equal protein loading. Peroxidase-conjugated secondary anti-rabbit at 1:2000 dilution (#sc-2004, Santa Cruz Biotechnology, Dallas, TX) was used, and bands were detected using SuperSignal West Pico Plus Chemiluminescent Substrate (#34580, Thermo Fisher Scientific). Densitometry analysis of immunoblots was performed using ImageJ software and normalized to loading control.

Transmission Electron Microscopy (TEM)

Cells were fixed with 2.5% glutaraldehyde in 0.1 M sodium cacodylate (pH 7.4) for 2 h at room temperature. Fixed cells were collected and post-fixed with 1% osmium tetroxide (OsO_4) in 0.1 M sodium cacodylate and counterstained in 1% uranyl nitrate. The pellets were dehydrated through a graduated acetone series and embedded in Epon 812 resin (#14120, Electron Microscopy Sciences, Hatfield, PA) for sectioning. From thin sections, ultrastructure of cells was observed under a transmission electron microscope (EM 109, Carl Zeiss, Oberkochen, Germany) and images were collected with a bottom-mount film-based camera. Mitophagy presence (autophagosomes enclosing mitochondria) was evaluated by morphometric analysis using TEM, where 50 cells per treatment were analyzed. Results were expressed as a percentage of mitophagy.

Parkinson's Disease Animal Model

C57BL/6J male mice (8–10 weeks old) (Circulo ADN, Mexico City) were subjected to intraperitoneal injections of 10 mg/kg paraquat or PBS three times per week for six consecutive weeks. For autophagy stimulation, rapamycin (1 mg/kg) was administered twice per week, 1 week before paraquat intoxication, and continued along with paraquat treatment in alternate days.

Mice were maintained on a 12-h light-dark cycle, with free access to Prolab RMH 2500 pellets (#5P14, LabDiet, St. Louis, MO) and water. Body weight of all mice was recorded daily. All experiments were conducted in accordance with the Mexican Official Norm "NOM-062-ZOO-1999" (De Aluja, 2002) and the Institutional Committee for the Care and Use of Laboratory Animals (Comite Institucional para el Cuidado y Uso de los Animales de Laboratorio, CICUAL), and approved by the Ethical Committee of our University (registration number HT17-00004).

Disability Score

The disability score was assessed individually in all mice at the end of the animal model, as a sum of gait and body posture abnormalities by direct visual inspection in their cages, as previously described [59, 90]. Before scoring, which was performed blinded, the normal behavior was observed in untreated mice for reference. Briefly, gait was scored as 0 = normal; 1 = slightly abnormal; 2 = severely abnormal with short steps and intermittent/staggered movements. Body posture was scored as 0 = normal; 1 = slightly abnormal/flexed; 2 = severely abnormal with curved posture [59, 90]. Both scores are added as a disability score, in which the maximal score is 4.

Nest Scoring

Mice were supplied with 5 g of compressed cotton squares, and behavior was evaluated based on a nest scoring system, as previously reported [61]. Briefly, nests were scored considering the height and closure of the walls surrounding the nest cavity. The higher scores indicate higher quality nests, equivalent to a normal behavior (score of 5 = complete dome-shaped nest), whereas those with lower scores were of poor quality and corresponded to an abnormal behavior (score of 4 = incomplete dome-shaped nest; score of 3 = cup-shaped nest; score of 2 = flat nest; and the scores of 1 and 0 refer to disturbed and undisturbed nesting material, respectively) [61].

Immunofluorescence

At the end of the experimental animal model, mice were anesthetized with an intramuscular injection of 10 mg/kg xylazine (#Q7833099, PiSA Labs, General Escobedo, Mexico) and 100 mg/kg ketamine (#Q7833028, PiSA Labs) followed by an intraperitoneal injection of sodium pentobarbital (88 mg/kg). Afterward, mice were perfused intracardially with 4% paraformaldehyde (PFA) in 0.1 M sodium phosphate buffer (pH 7.4). Brains were removed and post-fixed for 24 h in 4% PFA. Midbrains were cut into 5-μm coronal sections using a sliding microtome. Sections were blocked with 10% normal horse serum (#16050-122, Thermo Fisher Scientific) and incubated with rabbit anti-TH antibody (#ab112, Abcam) or mouse anti-IBA-1 (#ab15690, Abcam), overnight at 4 °C. After rinsing, sections were incubated with secondary Alexa 488 anti-rabbit (#ab150077, Abcam) or Alexa 594 anti-rabbit (#ab150080, Abcam) for 1 h at RT. Sections were mounted with VECTASHIELD Antifade Mounting Medium with DAPI. Images were collected on a Nikon Eclipse 50i fluorescent microscope and analyzed using ImageJ software. TH and IBA-1 positive cells counting was performed in four random fields per section.

Statistical Analysis

All experiment replicas were independent and performed on separate days. Collected data were analyzed according to statistical criteria by using paired or unpaired *t* test or two-way ANOVA, and the appropriate parametric or nonparametric normality post-test using statistical software (Prism 6, GraphPad Software, San Diego, CA). A probability value of $p < 0.05$ was considered statistically significant. Data were plotted as mean values of at least three independent experiments ± SEM using the same statistical package for data analysis. Plots and WB presented are representative of at least three independent experiments.

Acknowledgments This work was supported by the National Council of Science and Technology (Consejo Nacional de Ciencia y Tecnología, CONACYT: CB-2013-221615) and the Program for the Professional Development of the Professors (Programa para el Desarrollo Profesional Docente, PRODEP) (DSA/103.5/14/11021) to AGG. MJRM, APDJ, YGC, and AGA received a scholarship from CONACYT.

Compliance with Ethical Standards

Conflict of Interest The authors declare that they have no conflict of interest.

Ethical Approval All procedures performed in studies involving animals were following the Mexican Official Norm "NOM-062-ZOO-1999" (De Aluja, 2002) and our university's Institutional Animal Care and Use Committee (Comite Institucional para el Cuidado y Uso de los Animales de Laboratorio, CICUAL). This study was approved by the Ethical Committee of our University (registration number HT17-00004).

Author Contributions HRR and AGG conceived and designed the experiments. APDJ performed the experiments of cell death and oxidative stress. YGC performed the analyses of flow cytometry and TEM. MJRM and AGA performed the experiments in mice. MJRM, APDJ, YGC, AGA, MJLA, OSC, RMOL, HRR, and AGG analyzed the results. MJLA, OSC, RMOL, and HRR provided feedback on the manuscript. MJRM and AGG wrote the paper. All the authors reviewed and approved the final version of the manuscript.

References

1. Shults CW (2006) Lewy bodies. Proc Natl Acad Sci U S A 103(6): 1661–1668. https://doi.org/10.1073/pnas.0509567103
2. Hornykiewicz O (2006) The discovery of dopamine deficiency in the parkinsonian brain. J Neural Transm Suppl (70):9–15
3. Horowitz MP, Greenamyre JT (2010) Gene-environment interactions in Parkinson's disease: the importance of animal modeling. Clin Pharmacol Ther 88(4):467–474. https://doi.org/10.1038/clpt.2010.138
4. Vance JM, Ali S, Bradley WG, Singer C, Di Monte DA (2010) Gene-environment interactions in Parkinson's disease and other forms of parkinsonism. Neurotoxicology 31 (5):598–602. doi: https://doi.org/10.1016/j.neuro.2010.04.007
5. Elbaz A, Tranchant C (2007) Epidemiologic studies of environmental exposures in Parkinson's disease. J Neurol Sci 262(1–2):37–44. https://doi.org/10.1016/j.jns.2007.06.024
6. Franco R, Li S, Rodriguez-Rocha H, Burns M, Panayiotidis MI (2010) Molecular mechanisms of pesticide-induced neurotoxicity: Relevance to Parkinson's disease. Chem Biol Interact 188(2):289–300. https://doi.org/10.1016/j.cbi.2010.06.003
7. Checkoway H, Nelson LM (1999) Epidemiologic approaches to the study of Parkinson's disease etiology. Epidemiology 10(3):327–336
8. Tanner CM, Kamel F, Ross GW, Hoppin JA, Goldman SM, Korell M, Marras C, Bhudhikanok GS et al (2011) Rotenone, paraquat, and Parkinson's disease. Environ Health Perspect 119(6):866–872. https://doi.org/10.1289/ehp.1002839
9. Levy OA, Malagelada C, Greene LA (2009) Cell death pathways in Parkinson's disease: proximal triggers, distal effectors, and final steps. Apoptosis 14(4):478–500. https://doi.org/10.1007/s10495-008-0309-3
10. Bove J, Prou D, Perier C, Przedborski S (2005) Toxin-induced models of Parkinson's disease. NeuroRx 2(3):484–494. https://doi.org/10.1602/neurorx.2.3.484
11. Yao Z, Wood NW (2009) Cell death pathways in Parkinson's disease: role of mitochondria. Antioxid Redox Signal 11(9):2135–2149. https://doi.org/10.1089/ARS.2009.2624
12. Pollanen MS, Dickson DW, Bergeron C (1993) Pathology and biology of the Lewy body. J Neuropathol Exp Neurol 52(3):183–191
13. Cook C, Stetler C, Petrucelli L (2012) Disruption of protein quality control in Parkinson's disease. Cold Spring Harb Perspect Med 2(5):a009423. https://doi.org/10.1101/cshperspect.a009423
14. Ebrahimi-Fakhari D, Wahlster L, McLean PJ (2012) Protein degradation pathways in Parkinson's disease: curse or blessing. Acta Neuropathol 124(2):153–172. https://doi.org/10.1007/s00401-012-1004-6
15. Mazzulli JR, Zunke F, Isacson O, Studer L, Krainc D (2016) α-Synuclein-induced lysosomal dysfunction occurs through disruptions in protein trafficking in human midbrain synucleinopathy models. Proc Natl Acad Sci U S A 113(7):1931–1936. https://doi.org/10.1073/pnas.1520335113
16. Webb JL, Ravikumar B, Atkins J, Skepper JN, Rubinsztein DC (2003) Alpha-Synuclein is degraded by both autophagy and the proteasome. J Biol Chem 278(27):25009–25013. https://doi.org/10.1074/jbc.M300227200
17. Dunn WA (1994) Autophagy and related mechanisms of lysosome-mediated protein degradation. Trends Cell Biol 4(4):139–143
18. Klionsky DJ, Emr SD (2000) Autophagy as a regulated pathway of cellular degradation. Science 290(5497):1717–1721
19. He C, Klionsky DJ (2009) Regulation mechanisms and signaling pathways of autophagy. Annu Rev Genet 43:67–93. https://doi.org/10.1146/annurev-genet-102808-114910
20. Eskelinen EL (2005) Maturation of autophagic vacuoles in mammalian cells. Autophagy 1(1):1–10
21. Hara T, Nakamura K, Matsui M, Yamamoto A, Nakahara Y, Suzuki-Migishima R, Yokoyama M, Mishima K et al (2006) Suppression of basal autophagy in neural cells causes neurodegenerative disease in mice. Nature 441(7095):885–889. https://doi.org/10.1038/nature04724
22. Komatsu M, Waguri S, Chiba T, Murata S, Iwata J, Tanida I, Ueno T, Koike M et al (2006) Loss of autophagy in the central nervous system causes neurodegeneration in mice. Nature 441(7095):880–884. https://doi.org/10.1038/nature04723
23. Friedman LG, Lachenmayer ML, Wang J, He L, Poulose SM, Komatsu M, Holstein GR, Yue Z (2012) Disrupted autophagy leads to dopaminergic axon and dendrite degeneration and promotes presynaptic accumulation of α-synuclein and LRRK2 in the brain. J Neurosci 32(22):7585–7593. https://doi.org/10.1523/JNEUROSCI.5809-11.2012
24. Ahmed I, Liang Y, Schools S, Dawson VL, Dawson TM, Savitt JM (2012) Development and characterization of a new Parkinson's disease model resulting from impaired autophagy. J Neurosci 32(46): 16503–16509. https://doi.org/10.1523/JNEUROSCI.0209-12.2012

25. Anglade P, Vyas S, Javoy-Agid F, Herrero MT, Michel PP, Marquez J, Mouatt-Prigent A, Ruberg M et al (1997) Apoptosis and autophagy in nigral neurons of patients with Parkinson's disease. Histol Histopathol 12(1):25–31
26. Zhu JH, Guo F, Shelburne J, Watkins S, Chu CT (2003) Localization of phosphorylated ERK/MAP kinases to mitochondria and autophagosomes in Lewy body diseases. Brain Pathol 13(4):473–481
27. Rodriguez-Rocha H, Garcia-Garcia A, Pickett C, Li S, Jones J, Chen H, Webb B, Choi J et al (2013) Compartmentalized oxidative stress in dopaminergic cell death induced by pesticides and complex I inhibitors: distinct roles of superoxide anion and superoxide dismutases. Free Radic Biol Med 61C:370–383. https://doi.org/10.1016/j.freeradbiomed.2013.04.021
28. Garcia-Garcia A, Anandhan A, Burns M, Chen H, Zhou Y, Franco R (2013) Impairment of Atg5-dependent autophagic flux promotes paraquat- and MPP+-induced apoptosis but not rotenone or 6-hydroxydopamine toxicity. Toxicol Sci 136(166):182. https://doi.org/10.1093/toxsci/kft188
29. González-Polo RA, Niso-Santano M, Ortíz-Ortíz MA, Gómez-Martín A, Morán JM, García-Rubio L, Francisco-Morcillo J, Zaragoza C et al (2007) Inhibition of paraquat-induced autophagy accelerates the apoptotic cell death in neuroblastoma SH-SY5Y cells. Toxicol Sci 97(2):448–458. https://doi.org/10.1093/toxsci/kfm040
30. Wills J, Credle J, Oaks AW, Duka V, Lee JH, Jones J, Sidhu A (2012) Paraquat, but not maneb, induces synucleinopathy and tauopathy in striata of mice through inhibition of proteasomal and autophagic pathways. PLoS One 7(1):e30745. https://doi.org/10.1371/journal.pone.0030745
31. Scherz-Shouval R, Shvets E, Fass E, Shorer H, Gil L, Elazar Z (2007) Reactive oxygen species are essential for autophagy and specifically regulate the activity of Atg4. EMBO J 26(7):1749–1760. https://doi.org/10.1038/sj.emboj.7601623
32. Kubota C, Torii S, Hou N, Saito N, Yoshimoto Y, Imai H, Takeuchi T (2010) Constitutive reactive oxygen species generation from autophagosome/lysosome in neuronal oxidative toxicity. J Biol Chem 285(1):667–674. https://doi.org/10.1074/jbc.M109.053058
33. Chen Y, Azad MB, Gibson SB (2009) Superoxide is the major reactive oxygen species regulating autophagy. Cell Death Differ 16(7):1040–1052. https://doi.org/10.1038/cdd.2009.49
34. Wan FY, Wang YN, Zhang GJ (2001) The influence of oxidation of membrane thiol groups on lysosomal proton permeability. Biochem J 360(Pt 2):355–362
35. Bensaad K, Cheung EC, Vousden KH (2009) Modulation of intracellular ROS levels by TIGAR controls autophagy. EMBO J 28(19):3015–3026. https://doi.org/10.1038/emboj.2009.242
36. Jung CH, Ro SH, Cao J, Otto NM, Kim DH (2010) mTOR regulation of autophagy. FEBS Lett 584(7):1287–1295. https://doi.org/10.1016/j.febslet.2010.01.017
37. Noda T, Ohsumi Y (1998) Tor, a phosphatidylinositol kinase homologue, controls autophagy in yeast. J Biol Chem 273(7):3963–3966
38. Fei Q, McCormack AL, Di Monte DA, Ethell DW (2008) Paraquat neurotoxicity is mediated by a Bak-dependent mechanism. J Biol Chem 283(6):3357–3364. https://doi.org/10.1074/jbc.M708451200
39. Yang W, Tiffany-Castiglioni E, Koh HC, Son IH (2009) Paraquat activates the IRE1/ASK1/JNK cascade associated with apoptosis in human neuroblastoma SH-SY5Y cells. Toxicol Lett 191 (2–3):203–210. doi:https://doi.org/10.1016/j.toxlet.2009.08.024
40. Nuber S, Tadros D, Fields J, Overk CR, Ettle B, Kosberg K, Mante M, Rockenstein E et al (2014) Environmental neurotoxic challenge of conditional alpha-synuclein transgenic mice predicts a dopaminergic olfactory-striatal interplay in early PD. Acta Neuropathol 127(4):477–494. https://doi.org/10.1007/s00401-014-1255-5
41. Suzuki J, Denning DP, Imanishi E, Horvitz HR, Nagata S (2013) Xk-related protein 8 and CED-8 promote phosphatidylserine exposure in apoptotic cells. Science 341(6144):403–406. https://doi.org/10.1126/science.1236758
42. Suzuki J, Imanishi E, Nagata S (2014) Exposure of phosphatidylserine by Xk-related protein family members during apoptosis. J Biol Chem 289(44):30257–30267. https://doi.org/10.1074/jbc.M114.583419
43. Suzuki J, Imanishi E, Nagata S (2016) Xkr8 phospholipid scrambling complex in apoptotic phosphatidylserine exposure. Proc Natl Acad Sci U S A 113(34):9509–9514. https://doi.org/10.1073/pnas.1610403113
44. Rhee SG, Woo HA (2011) Multiple functions of peroxiredoxins: peroxidases, sensors and regulators of the intracellular messenger H2O2, and protein chaperones. Antioxid Redox Signal 15(3):781–794. https://doi.org/10.1089/ars.2010.3393
45. Bryk R, Griffin P, Nathan C (2000) Peroxynitrite reductase activity of bacterial peroxiredoxins. Nature 407(6801):211–215. https://doi.org/10.1038/35025109
46. Rhee SG, Woo HA, Kil IS, Bae SH (2012) Peroxiredoxin functions as a peroxidase and a regulator and sensor of local peroxides. J Biol Chem 287(7):4403–4410. https://doi.org/10.1074/jbc.R111.283432
47. Lei S, Zavala-Flores L, Garcia-Garcia A, Nandakumar R, Huang Y, Madayiputhiya N, Stanton RC, Dodds ED et al (2014) Alterations in energy/redox metabolism induced by mitochondrial and environmental toxins: a specific role for glucose-6-phosphate-dehydrogenase and the pentose phosphate pathway in paraquat toxicity. ACS Chem Biol 9(9):2032–2048. https://doi.org/10.1021/cb400894a
48. Lee YM, Park SH, Shin DI, Hwang JY, Park B, Park YJ, Lee TH, Chae HZ et al (2008) Oxidative modification of peroxiredoxin is associated with drug-induced apoptotic signaling in experimental models of Parkinson disease. J Biol Chem 283(15):9986–9998. https://doi.org/10.1074/jbc.M800426200
49. Roede JR, Hansen JM, Go YM, Jones DP (2011) Maneb and paraquat-mediated neurotoxicity: involvement of peroxiredoxin/thioredoxin system. Toxicol Sci 121(2):368–375. https://doi.org/10.1093/toxsci/kfr058
50. Woo HA, Kang SW, Kim HK, Yang KS, Chae HZ, Rhee SG (2003) Reversible oxidation of the active site cysteine of peroxiredoxins to cysteine sulfinic acid. Immunoblot detection with antibodies specific for the hyperoxidized cysteine-containing sequence. J Biol Chem 278(48):47361–47364. https://doi.org/10.1074/jbc.C300428200
51. Eskelinen EL (2008) Fine structure of the autophagosome. Methods Mol Biol 445:11–28. https://doi.org/10.1007/978-1-59745-157-4_2
52. Loos B, du Toit A, Hofmeyr JH (2014) Defining and measuring autophagosome flux—Concept and reality. Autophagy 10(11):2087–2096. https://doi.org/10.4161/15548627.2014.973338
53. Poole B, Ohkuma S (1981) Effect of weak bases on the intralysosomal pH in mouse peritoneal macrophages. J Cell Biol 90(3):665–669
54. Glaumann H, Ahlberg J (1987) Comparison of different autophagic vacuoles with regard to ultrastructure, enzymatic composition, and degradation capacity–formation of crinosomes. Exp Mol Pathol 47(3):346–362
55. Liu H, Dai C, Fan Y, Guo B, Ren K, Sun T, Wang W (2017) From autophagy to mitophagy: the roles of P62 in neurodegenerative diseases. J Bioenerg Biomembr 49(5):413–422. https://doi.org/10.1007/s10863-017-9727-7
56. Jankovic J (2008) Parkinson's disease: clinical features and diagnosis. J Neurol Neurosurg Psychiatry 79(4):368–376. https://doi.org/10.1136/jnnp.2007.131045

57. Bloem BR, Hausdorff JM, Visser JE, Giladi N (2004) Falls and freezing of gait in Parkinson's disease: a review of two interconnected, episodic phenomena. Mov Disord 19(8):871–884. https://doi.org/10.1002/mds.20115
58. Giladi N, Treves TA, Simon ES, Shabtai H, Orlov Y, Kandinov B, Paleacu D, Korczyn AD (2001) Freezing of gait in patients with advanced Parkinson's disease. J Neural Transm (Vienna) 108(1):53–61. https://doi.org/10.1007/s007020170096
59. Sager TN, Kirchhoff J, Mørk A, Van Beek J, Thirstrup K, Didriksen M, Lauridsen JB (2010) Nest building performance following MPTP toxicity in mice. Behav Brain Res 208(2):444–449. https://doi.org/10.1016/j.bbr.2009.12.014
60. Deacon RM (2006) Assessing nest building in mice. Nat Protoc 1(3):1117–1119. https://doi.org/10.1038/nprot.2006.170
61. Hess SE, Rohr S, Dufour BD, Gaskill BN, Pajor EA, Garner JP (2008) Home improvement: C57BL/6J mice given more naturalistic nesting materials build better nests. J Am Assoc Lab Anim Sci 47(6):25–31
62. McGeer PL, McGeer EG (2008) Glial reactions in Parkinson's disease. Mov Disord 23(4):474–483. https://doi.org/10.1002/mds.21751
63. Purisai MG, McCormack AL, Cumine S, Li J, Isla MZ, Di Monte DA (2007) Microglial activation as a priming event leading to paraquat-induced dopaminergic cell degeneration. Neurobiol Dis 25(2):392–400. https://doi.org/10.1016/j.nbd.2006.10.008
64. Cicchetti F, Lapointe N, Roberge-Tremblay A, Saint-Pierre M, Jimenez L, Ficke BW, Gross RE (2005) Systemic exposure to paraquat and maneb models early Parkinson's disease in young adult rats. Neurobiol Dis 20(2):360–371. https://doi.org/10.1016/j.nbd.2005.03.018
65. Dong X, Milholland B, Vijg J (2016) Evidence for a limit to human lifespan. Nature 538(7624):257–259. https://doi.org/10.1038/nature19793
66. Arduíno DM, Esteves AR, Cortes L, Silva DF, Patel B, Grazina M, Swerdlow RH, Oliveira CR et al (2012) Mitochondrial metabolism in Parkinson's disease impairs quality control autophagy by hampering microtubule-dependent traffic. Hum Mol Genet 21(21):4680–4702. https://doi.org/10.1093/hmg/dds309
67. Radad K, Moldzio R, Rausch WD (2015) Rapamycin protects dopaminergic neurons against rotenone-induced cell death in primary mesencephalic cell culture. Folia Neuropathol 53(3):250–261
68. Pan T, Rawal P, Wu Y, Xie W, Jankovic J, Le W (2009) Rapamycin protects against rotenone-induced apoptosis through autophagy induction. Neuroscience 164(2):541–551. https://doi.org/10.1016/j.neuroscience.2009.08.014
69. Mouatt-Prigent A, Karlsson JO, Agid Y, Hirsch EC (1996) Increased M-calpain expression in the mesencephalon of patients with Parkinson's disease but not in other neurodegenerative disorders involving the mesencephalon: a role in nerve cell death? Neuroscience 73(4):979–987
70. Crocker SJ, Smith PD, Jackson-Lewis V, Lamba WR, Hayley SP, Grimm E, Callaghan SM, Slack RS et al (2003) Inhibition of calpains prevents neuronal and behavioral deficits in an MPTP mouse model of Parkinson's disease. J Neurosci 23(10):4081–4091
71. Samantaray S, Butler JT, Ray SK, Banik NL (2008) Extranigral neurodegeneration in Parkinson's disease. Ann N Y Acad Sci 1139:331–336. https://doi.org/10.1196/annals.1432.002
72. Esteves AR, Arduíno DM, Swerdlow RH, Oliveira CR, Cardoso SM (2010) Dysfunctional mitochondria uphold calpain activation: Contribution to Parkinson's disease pathology. Neurobiol Dis 37(3):723–730. https://doi.org/10.1016/j.nbd.2009.12.011
73. Jiang J, Zuo Y, Gu Z (2013) Rapamycin protects the mitochondria against oxidative stress and apoptosis in a rat model of Parkinson's disease. Int J Mol Med 31(4):825–832. https://doi.org/10.3892/ijmm.2013.1280
74. Das A, Durrant D, Koka S, Salloum FN, Xi L, Kukreja RC (2014) Mammalian target of rapamycin (mTOR) inhibition with rapamycin improves cardiac function in type 2 diabetic mice: potential role of attenuated oxidative stress and altered contractile protein expression. J Biol Chem 289(7):4145–4160. https://doi.org/10.1074/jbc.M113.521062
75. Sun DZ, Song CQ, Xu YM, Wang R, Liu W, Liu Z, Dong XS (2018) Involvement of PINK1/Parkin-mediated mitophagy in paraquat- induced apoptosis in human lung epithelial-like A549 cells. Toxicol in Vitro 53:148–159. https://doi.org/10.1016/j.tiv.2018.08.009
76. Brooks AI, Chadwick CA, Gelbard HA, Cory-Slechta DA, Federoff HJ (1999) Paraquat elicited neurobehavioral syndrome caused by dopaminergic neuron loss. Brain Res 823(1–2):1–10
77. Majumder S, Richardson A, Strong R, Oddo S (2011) Inducing autophagy by rapamycin before, but not after, the formation of plaques and tangles ameliorates cognitive deficits. PLoS One 6(9):e25416. https://doi.org/10.1371/journal.pone.0025416
78. Thiruchelvam M, Richfield EK, Baggs RB, Tank AW, Cory-Slechta DA (2000) The nigrostriatal dopaminergic system as a preferential target of repeated exposures to combined paraquat and maneb: implications for Parkinson's disease. J Neurosci 20(24):9207–9214
79. Peng J, Mao XO, Stevenson FF, Hsu M, Andersen JK (2004) The herbicide paraquat induces dopaminergic nigral apoptosis through sustained activation of the JNK pathway. J Biol Chem 279(31):32626–32632. https://doi.org/10.1074/jbc.M404596200
80. McCormack AL, Thiruchelvam M, Manning-Bog AB, Thiffault C, Langston JW, Cory-Slechta DA, Di Monte DA (2002) Environmental risk factors and Parkinson's disease: selective degeneration of nigral dopaminergic neurons caused by the herbicide paraquat. Neurobiol Dis 10(2):119–127
81. Malagelada C, Jin ZH, Jackson-Lewis V, Przedborski S, Greene LA (2010) Rapamycin protects against neuron death in in vitro and in vivo models of Parkinson's disease. J Neurosci 30(3):1166–1175. https://doi.org/10.1523/JNEUROSCI.3944-09.2010
82. Liu K, Shi N, Sun Y, Zhang T, Sun X (2013) Therapeutic effects of rapamycin on MPTP-induced parkinsonism in mice. Neurochem Res 38(1):201–207. https://doi.org/10.1007/s11064-012-0909-8
83. McGeer PL, Schwab C, Parent A, Doudet D (2003) Presence of reactive microglia in monkey substantia nigra years after 1-methyl-4-phenyl-1,2,3,6-tetrahydropyridine administration. Ann Neurol 54(5):599–604. https://doi.org/10.1002/ana.10728
84. Barcia C, Sánchez Bahillo A, Fernández-Villalba E, Bautista V, Poza Y, Poza M, Fernández-Barreiro A, Hirsch EC et al (2004) Evidence of active microglia in substantia nigra pars compacta of parkinsonian monkeys 1 year after MPTP exposure. Glia 46(4):402–409. https://doi.org/10.1002/glia.20015
85. Sugama S, Yang L, Cho BP, DeGiorgio LA, Lorenzl S, Albers DS, Beal MF, Volpe BT et al (2003) Age-related microglial activation in 1-methyl-4-phenyl-1,2,3,6-tetrahydropyridine (MPTP)-induced dopaminergic neurodegeneration in C57BL/6 mice. Brain Res 964(2):288–294
86. Cicchetti F, Brownell AL, Williams K, Chen YI, Livni E, Isacson O (2002) Neuroinflammation of the nigrostriatal pathway during progressive 6-OHDA dopamine degeneration in rats monitored by immunohistochemistry and PET imaging. Eur J Neurosci 15(6):991–998
87. Depino AM, Earl C, Kaczmarczyk E, Ferrari C, Besedovsky H, del Rey A, Pitossi FJ, Oertel WH (2003) Microglial activation with atypical proinflammatory cytokine expression in a rat model of Parkinson's disease. Eur J Neurosci 18(10):2731–2742

88. Sherer TB, Betarbet R, Kim JH, Greenamyre JT (2003) Selective microglial activation in the rat rotenone model of Parkinson's disease. Neurosci Lett 341(2):87–90
89. Lu M, Su C, Qiao C, Bian Y, Ding J, Hu G (2016) Metformin prevents dopaminergic neuron death in MPTP/P-induced mouse model of Parkinson's disease via autophagy and mitochondrial ROS clearance. Int J Neuropsychopharmacol 19(9):pyw047. https://doi.org/10.1093/ijnp/pyw047
90. Kirchhoff J, Mørk A, Brennum LT, Sager TN (2009) Striatal extracellular dopamine levels and behavioural reversal in MPTP-lesioned mice. Neuroreport 20(5):482–486. https://doi.org/10.1097/WNR.0b013e32832984d6